

The Muon and Tau Electric Dipole Moments in the B-L Supersymmetric Standard Model

Wen-Hui Zhang,^{1,2,3,*} Jin-Lei Yang,^{1,2,3,†} Zhao-Feng Ge,^{4,5} Yu-Li Yan,^{1,2,3} and Yin-Jie Zhang^{1,2,3}

¹*Department of Physics, Hebei University, Baoding, 071002, China*

²*Key Laboratory of High-precision Computation and Application of Quantum Field Theory of Hebei Province, Baoding, 071002, China*

³*Research Center for Computational Physics of Hebei Province, Baoding, 071002, China*

⁴*Radiation Monitoring Technical Center of Ministry of Ecology and Environment*

⁵*Key Laboratory of Radiation Environmental Monitoring, Ministry of Ecology and Environment*

Abstract

Recently proposed experiments are expected to significantly improve the measurement sensitivities of the electric dipole moments (EDMs) of muon (d_μ) and tau (d_τ). Given that theoretical predictions for d_μ and d_τ typically surpass those for the electron EDM, this work focuses on studying the contributions from the CP-violating (CPV) effects in the B-L supersymmetric (SUSY) standard model (B-LSSM) to d_μ and d_τ . After considering the corrections from some two-loop diagrams, the contributions in the B-LSSM to the EDMs of charged leptons are presented analytically in general forms. The numerical results show that the traditional μ -term in most SUSY models makes dominant contributions to d_μ and d_τ , while the B-LSSM specific CPV parameters also induce significant effects. It is found that across a substantial region of the B-LSSM parameter space, d_μ falls well within the projected sensitivity at Phase II of the proposed experiment, and $|d_\tau|$ can reach about $10^{-21}e \cdot \text{cm}$.

* zwh_0218@163.com

† jlyang@hbu.edu.cn

I. INTRODUCTION

The CP-violating (CPV) phases in Cabibbo-Kobayashi-Maskawa (CKM) matrix, which constitute the sole sources of CPV in the standard model (SM), have been observed precisely [1–3]. However, the contributions from the SM CPV interactions to the baryon asymmetry of the universe are too tiny to account for the experimental observations [4, 5]. Consequently, the introduction of new CPV sources in the new physics (NP) models is imperative. These new CPV sources may make significant contributions to the electric dipole moment (EDM) of a fundamental particle, which are highly suppressed by the small CKM phases in the SM [6–10]. This implies that the observations of non-zero fundamental particle EDMs would represent an unambiguous signal of NP [11, 12], and corresponding theoretical studies may shed critical light on the origin of CPV.

Generally, most NP models predict the existence of new CPV sources and consequently large contributions to EDMs. For instance, the EDMs of electron, neutron and mercury have been extensively analyzed within the minimal supersymmetry (SUSY) model [13–15]. The contributions in the minimal Left-Right model to the neutron and electron EDMs are studied in Ref. [16, 17]. Predictions for the electron EDM in the complex two-Higgs doublet model are presented in Ref. [18], where contributions from two-loop Barr-Zee diagrams [19] are also included [20]. In the Next-to-Minimal SUSY model, the prospects of measuring extra CPV sources through their contributions to EDMs are investigated [21]. Various two-loop contributions in the MSSM with R -parity violation are evaluated in Refs. [22–25]. In the $U(1)_{B-L}$ extended MSSM (B-LSSM) [26–35], where B , L represent baryon and lepton number respectively, we have previously explored the contributions from new CPV sources to the EDMs of neutron and heavy quarks [36], as well as to the electron EDM and electroweak baryogenesis [37], the cancellations between different contributions of CPV phases are also analyzed.

Compared to the constraints on the EDMs of neutron, mercury and electron, the experimental constraints on the τ and μ lepton EDM d_τ , d_μ are weaker due to the short lifetimes of them. The most stringent upper bound on d_τ is provided by the Belle II Collaboration as $-1.85 \times 10^{-17} e \cdot \text{cm} < d_\tau < 0.61 \times 10^{-17} e \cdot \text{cm}$ [38], while the corresponding limit on d_μ is reported by the BNL muon $g - 2$ experiment as $|d_\mu| < 1.9 \times 10^{-19} e \cdot \text{cm}$ [39]. Both limits are much weaker than the constraint on the electron EDM, $|d_e| < 4.1 \times 10^{-30} e \cdot \text{cm}$ [40].

However, ongoing and projected experiments have the potential to improve the sensitivity to d_τ , which can reach [41–50].

$$d_\tau < 10^{-19} e \cdot \text{cm} \quad (1)$$

Furthermore, utilizing the frozen-spin technique within a compact storage trap, a new experiment has been recently proposed to measure d_μ , with expected sensitivities reaching [51, 52]:

$$\begin{aligned} d_\mu &< 3 \times 10^{-21} e \cdot \text{cm} \quad (\text{Phase I}), \\ d_\mu &< 6 \times 10^{-23} e \cdot \text{cm} \quad (\text{Phase II}). \end{aligned} \quad (2)$$

Consequently, there is strong motivation to extend theoretical investigations of EDMs to d_τ and d_μ within NP models, where these observables may be enhanced to levels accessible by next generation experiments. For instance, Ref. [53] computes and analyzes predictions for d_τ within two benchmark models featuring different hypercharge assignments. Additionally, the contributions from light axion-like couplings of τ to d_τ are also analyzed [54], they found the predicted d_τ approaches current experimental sensitivities and will be accessible to future measurements. Similarly, Ref. [55] utilizes the current upper bound and future projected sensitivity of d_μ to constrain dimension-six CP-violating operators within the SM effective field theory.

Based on our previous analyses of the neutron, heavy quarks, and electron EDMs within the B-LSSM, and motivated by the anticipated improvements in experimental sensitivities to d_μ and d_τ , this work focuses on investigating the contributions from new CPV sources in the B-LSSM to these leptonic EDMs. Compared to the MSSM, the local gauge symmetry of the B-LSSM is extended by $U(1)_{B-L}$, introducing an additional Z' gauge boson that can contribute to d_μ and d_τ at the two-loop level. Since the additional local gauge group is associated with the lepton number and the newly introduced scalar singlets acquire non-zero vacuum expectation values (VEVs), the observed neutrino oscillations can be naturally explained via the so-called Type-I seesaw mechanism [56, 57]. In addition, the superpartners of these new scalar singlets can also serve as viable dark matter candidates [58]. The MSSM predictions are now challenged by experiments, while the ones of B-LSSM can be relaxed significantly due to the additional structure. All these indicate that the B-LSSM is more attractive than the MSSM both theoretically and experimentally. Therefore, this work comprehensively explores the constraints imposed by the current upper bounds on d_μ and

d_τ upon the B-LSSM parameter space, and accesses whether the predicted EDMs fall within the reach of future experimental measurements.

The paper is organized as follows: In Sec. II, the relevant mass matrices and interactions in the B-LSSM are introduced, and the contributions to charged lepton EDMs are calculated analytically. The numerical results are presented and analyzed in Sec. III. A brief summary is given in Sec. IV. The lengthy formulae are collected in the Appendix.

II. THE B-LSSM AND CALCULATIONS OF d_l

In this section, we outline the relevant framework of the B-LSSM and present the analytical calculations for the charged lepton EDMs, d_l .

A. The relevant mass matrices and interactions

The scalar sector of the B-LSSM is extended by two scalar singlets

$$\eta \sim (1, 1, 0, -1), \quad \bar{\eta} \sim (1, 1, 0, 1), \quad (3)$$

where the charges in the brackets denote the quantum numbers under $SU(3)_C$, $SU(2)_L$, $U(1)_Y$, $U(1)_{B-L}$, respectively. The additional $U(1)_{B-L}$ local gauge symmetry is spontaneously broken when the two scalar singlet fields acquire non-zero VEVs:

$$\eta = \frac{1}{\sqrt{2}}(u_\eta + \phi_\eta + i\sigma_\eta), \quad \bar{\eta} = \frac{1}{\sqrt{2}}(u_{\bar{\eta}} + \phi_{\bar{\eta}} + i\sigma_{\bar{\eta}}). \quad (4)$$

where $\tan \beta' \equiv u_{\bar{\eta}}/u_\eta$ and $u^2 \equiv u_\eta^2 + u_{\bar{\eta}}^2$. The spontaneous breaking of $U(1)_{B-L}$ generates Majorana masses for the right-handed neutrinos. By combining these with the Dirac masses arising from the Higgs doublet VEVs, the Type-I seesaw mechanism is naturally realized.

At the one-loop level, the dominant contributions to d_μ and d_τ come from diagrams mediated by sleptons-neutralinos and charginos-sneutrinos in the loop. The slepton mass matrix can be written as

$$m_l^2 = \begin{pmatrix} m_{lL}^2, & \frac{1}{\sqrt{2}}Y_e^\dagger(v_1 A_l^\dagger - v_2 \mu) \\ \frac{1}{\sqrt{2}}Y_e(v_1 A_l - v_2 \mu^*), & m_{lR}^2 \end{pmatrix}, \quad (5)$$

where

$$\begin{aligned}
m_{\tilde{l}_L}^2 &= \frac{1}{8} \left[(g_1^2 + g_{YB}^2 - g_2^2 + g_B g_{YB})(v_1^2 - v_2^2) + 2g_B(g_B + g_{YB})(u_\eta^2 - u_{\bar{\eta}}^2) \right] \\
&\quad + m_{\tilde{l}}^2 + \frac{1}{2} v_1^2 Y_e Y_e^\dagger, \\
m_{\tilde{l}_R}^2 &= \frac{1}{8} \left[(2g_1^2 + 2g_{YB}^2 + g_B g_{YB})(v_2^2 - v_1^2) + 2g_B(g_B + 2g_{YB})(u_\eta^2 - u_{\bar{\eta}}^2) \right] \\
&\quad + m_{\tilde{e}}^2 + \frac{1}{2} v_1^2 Y_e Y_e^\dagger.
\end{aligned} \tag{6}$$

Similar to the MSSM, g_1 and g_2 are the standard gauge coupling constants, v_1, v_2 are the VEVs of the Higgs doublets, A_l denotes the trilinear coupling constant, μ is the μ term coupling, $m_{\tilde{l}}, m_{\tilde{e}}$ are the soft SUSY-breaking mass terms. Additionally, Y_e is the Yukawa coupling matrix of charged leptons. Furthermore, g_B is the gauge coupling constant associated with $U(1)_{B-L}$, and g_{YB} is the gauge coupling arising from the gauge kinetic mixing [59–64]. The squared mass matrices for CP-odd and CP-even sneutrinos can be written as

$$m_{\tilde{\nu}_{\text{odd}, \tilde{\nu}_{\text{even}}}}^2 = \begin{pmatrix} m_{\tilde{\nu}_L}^2, & \frac{1}{\sqrt{2}} v_2 \mathcal{R}(A_\nu) \\ \frac{1}{\sqrt{2}} v_2 \mathcal{R}(A_\nu), & m_{\tilde{\nu}_{\text{odd}, \text{even}R}}^2 \end{pmatrix}, \tag{7}$$

where

$$\begin{aligned}
m_{\tilde{\nu}_L}^2 &= \frac{1}{8} \left[(g_1^2 + g_{YB}^2 + g_2^2 + g_B g_{YB})(v_1^2 - v_2^2) + 2g_B(g_B + g_{YB})(u_\eta^2 - u_{\bar{\eta}}^2) \right] + m_{\tilde{l}}^2, \\
m_{\tilde{\nu}_{\text{odd}, \text{even}R}}^2 &= \frac{1}{8} \left[g_B g_{YB}(v_2^2 - v_1^2) + 2g_B^2(u_\eta^2 - u_{\bar{\eta}}^2) \right] - \sqrt{2} \left[u_\eta \mathcal{R}(A_R) - \sqrt{2} u_\eta^2 Y_R^\dagger Y_R \right] \\
&\quad + m_{\tilde{\nu}}^2 \pm \sqrt{2} u_{\bar{\eta}} \mathcal{R}(Y_R \mu_\eta^*).
\end{aligned} \tag{8}$$

Here, the \pm signs correspond to CP-odd and CP-even sneutrinos respectively. \mathcal{R} denotes the real part. Y_R is the Majorana coupling matrix of right-handed neutrinos while the Dirac coupling matrix is taken to be zero for simplicity. A_ν, A_R denote the relevant trilinear coupling constants. It is worth noting that all matrix elements of the sneutrinos are real; therefore, they do not significantly affect the numerical results for d_μ and d_τ . To simplify the parameter space, we take $Y_R = \text{diag}(0.1, 0.1, 0.1)$, $A_\nu = A_R = \text{diag}(0.1, 0.1, 0.1)$ TeV in the following computations.

The mass matrix of charginos in the B-LSSM is same as the one in the MSSM, while the

mass matrix of neutralinos on the basis $(\tilde{\lambda}_B, \tilde{\lambda}_W, \tilde{\lambda}_{H_d^0}, \tilde{\lambda}_{H_u^0}, \tilde{\lambda}_{B'}, \tilde{\lambda}_\eta, \tilde{\lambda}_{\bar{\eta}})$ can be written as

$$m_{\tilde{\chi}^0} = \begin{pmatrix} M_1 & 0 & -\frac{1}{2}g_1v_1 & \frac{1}{2}g_1v_2 & M_{BB'} & 0 & 0 \\ 0 & M_2 & \frac{1}{2}g_2v_1 & -\frac{1}{2}g_2v_2 & 0 & 0 & 0 \\ -\frac{1}{2}g_1v_1 & \frac{1}{2}g_2v_1 & 0 & -\mu & -\frac{1}{2}g_{YB}v_1 & 0 & 0 \\ \frac{1}{2}g_1v_2 & -\frac{1}{2}g_2v_2 & -\mu & 0 & \frac{1}{2}g_{YB}v_2 & 0 & 0 \\ M_{BB'} & 0 & -\frac{1}{2}g_{YB}v_1 & \frac{1}{2}g_{YB}v_2 & M_{BL} & -g_Bu_\eta & g_Bu_{\bar{\eta}} \\ 0 & 0 & 0 & 0 & -g_Bu_\eta & 0 & -\mu_\eta \\ 0 & 0 & 0 & 0 & g_Bu_{\bar{\eta}} & -\mu_\eta & 0 \end{pmatrix}. \quad (9)$$

Obviously, there are three additional neutralinos in the B-LSSM, which can make contributions to d_μ and d_τ at the one-loop level. Correspondingly, there are also three new CPV sources $M_{BB'}$, M_{BL} , μ_η in the model, they can affect the theoretical predictions on d_μ , d_τ through the one-loop level contributions.

The new scalars and Z' gauge boson can also contribute to the charged lepton EDMs through the Barr-Zee diagrams. The squared Higgs mass matrix after considering the two-loop effective potential corrections from top and stop quarks can be found in our previous work [65], which is used to carry out the numerical computations. The squared mass of new gauge boson Z' can be estimated by

$$M_{Z'} \approx \frac{1}{2}g_Bu, \quad (10)$$

where the terms proportional to v are neglected. All involved coupling constants are collected in the Appendix.

B. The contributions to d_l in the model

The effective Lagrangian for the charged lepton EDMs is described by the following operator:

$$\mathcal{L}_{\text{eff}} = -\frac{d_l}{2}(\bar{l}\sigma^{\mu\nu}i\gamma_5l)F_{\mu\nu} \quad (11)$$

where $l = e, \mu, \tau$ denote the charged lepton fields, $\sigma^{\mu\nu} = i[\gamma^\mu, \gamma^\nu]/2$ with γ^μ being the Dirac matrix, and $F_{\mu\nu}$ is the electromagnetic field strength tensor. The leading order contributions to d_l in the B-LSSM arise from the one-loop diagrams, which are plotted in Fig. 1. The

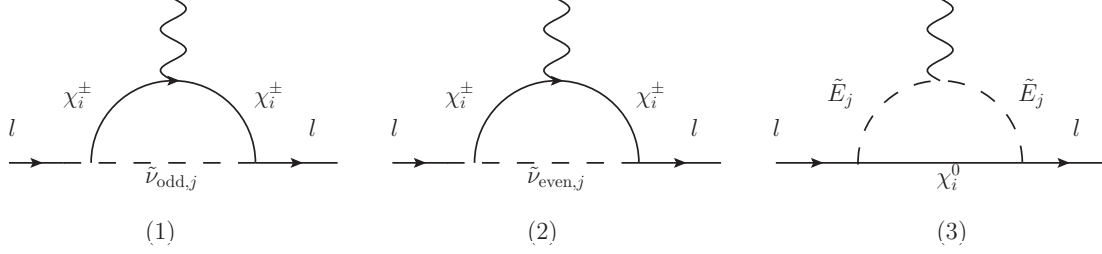


FIG. 1. The one-loop level diagrams contributing to the charged lepton EDMs.

resulting exoressions can be written as [66]

$$d_l^{(1)} = \sum_{i,j} \frac{-eM_{\chi_i^\pm}}{16\pi^2 M_{\nu_{\text{odd},j}}^2} \mathcal{I} \left(C_{\tilde{l}\chi_i^\pm \nu_{\text{odd},j}}^L C_{\tilde{l}\chi_i^\pm \nu_{\text{odd},j}}^R \right) f_1 \left(\frac{M_{\chi_i^\pm}^2}{M_{\nu_{\text{odd},j}}^2} \right), \quad (12)$$

$$d_l^{(2)} = \sum_{i,j} \frac{-eM_{\chi_i^\pm}}{16\pi^2 M_{\nu_{\text{even},j}}^2} \mathcal{I} \left(C_{\tilde{l}\chi_i^\pm \nu_{\text{even},j}}^L C_{\tilde{l}\chi_i^\pm \nu_{\text{even},j}}^R \right) f_1 \left(\frac{M_{\chi_i^\pm}^2}{M_{\nu_{\text{even},j}}^2} \right), \quad (13)$$

$$d_l^{(3)} = \sum_{i,j} \frac{-eM_{\chi_i^0}}{16\pi^2 M_{\tilde{E}_j}^2} \mathcal{I} \left(C_{\tilde{l}\chi_i^0 \tilde{E}_j}^L C_{\tilde{l}\chi_i^0 \tilde{E}_j}^R \right) f_2 \left(\frac{M_{\chi_i^0}^2}{M_{\tilde{E}_j}^2} \right), \quad (14)$$

where \mathcal{I} denotes the imaginary part, $M_{\nu_{\text{odd}}}$, $M_{\nu_{\text{even}}}$, M_{χ^\pm} , M_{χ^0} , $M_{\tilde{E}}$ denote the physical masses of the CP-odd sneutrinos, CP-even sneutrinos, charginos, neutralinos and sleptons, respectively. Furthermore, $C_{XYZ}^{L(R)}$ denotes the left (right)-handed coupling constant of the interactions between XYZ which can be found in the Appendix, and

$$f_1(x) = \frac{1}{2(1-x)^2} \left[3 - x + \frac{2 \ln x}{1-x} \right], \quad (15)$$

$$f_2(x) = \frac{1}{2(1-x)^2} \left[1 + x + \frac{2x \ln x}{1-x} \right]. \quad (16)$$

The two-loop level contributions to d_l considered in this work are plotted in Fig. 2, where the external photon is attached in all possible ways. Clearly, the new scalars and Z' gauge boson can also make contributions, and the resulting d_l can be correspondingly written as [67, 68]

$$d_l^{(a)-\gamma} = \frac{-e^2 m_l}{16\pi^4} \sum_{i,j,k} \mathcal{I} \left(C_{h_k \tilde{\chi}_i^\pm \chi_j^\pm} C_{h_k \tilde{l}}^* \right) \left[\ln \left(\frac{M_{h_k}^2}{m_l^2} \right) - 2 + \frac{m_l^2}{M_{h_k}^2} \Phi \left(\frac{m_l^2}{M_{h_k}^2} \right) \right] \frac{1}{M_{h_k}^2}, \quad (17)$$

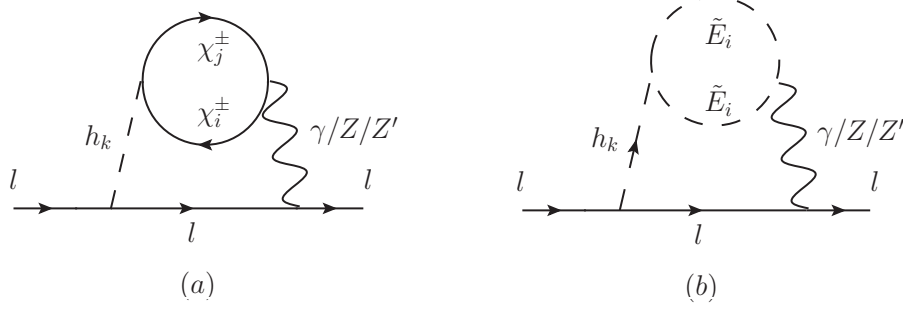


FIG. 2. The considered two-loop level diagrams contributing to the charged lepton EDMs, where photon is attached by all possible ways.

$$d_l^{(a)-Z} = \frac{-e^2 m_l}{64\pi^4} \sum_{i,j,k} \mathcal{I} \left[C_{h_k \bar{\chi}_i^\pm \chi_j^\pm} C_{h_k \bar{l} l}^* (C_{Z\bar{l}l}^L + C_{Z\bar{l}l}^R) (C_{Z\bar{\chi}_i^\pm \chi_j^\pm}^L + C_{Z\bar{\chi}_i^\pm \chi_j^\pm}^R) \right] \frac{1}{M_{h_k}^2} \times \left[\ln \left(\frac{M_{h_k}^2}{M_Z^2} \right) - \frac{m_l^2}{M_Z^2} \Phi \left(\frac{m_l^2}{M_Z^2} \right) + \frac{m_l^2}{M_{h_k}^2} \Phi \left(\frac{m_l^2}{M_{h_k}^2} \right) \right], \quad (18)$$

$$d_l^{(b)-\gamma} = \frac{-e^2}{128\pi^4} \sum_{i,k} \mathcal{I} \left(C_{h_k \tilde{E}_i \tilde{E}_i} C_{h_k \bar{l} l}^* \right) \left[\ln \left(\frac{M_{h_k}^2}{M_{\tilde{E}_i}^2} \right) + \frac{M_{\tilde{E}_i}^2}{M_{h_k}^2} \Phi \left(\frac{M_{\tilde{E}_i}^2}{M_{h_k}^2} \right) \right] \frac{1}{M_{h_k}^2}, \quad (19)$$

$$d_l^{(b)-Z} = \frac{-e}{128\pi^4} \sum_{i,k} \mathcal{I} \left[C_{h_k \tilde{E}_i \tilde{E}_i} C_{h_k \bar{l} l}^* C_{Z \tilde{E}_i \tilde{E}_i} (C_{Z\bar{l}l}^L + C_{Z\bar{l}l}^R) \right] \frac{1}{M_{h_k}^2 - M_Z^2} \times \left[\ln \left(\frac{M_{h_k}^2}{M_Z^2} \right) - \frac{M_{\tilde{E}_i}^2}{M_Z^2} \Phi \left(\frac{M_{\tilde{E}_i}^2}{M_Z^2} \right) + \frac{M_{\tilde{E}_i}^2}{M_{h_k}^2} \Phi \left(\frac{M_{\tilde{E}_i}^2}{M_{h_k}^2} \right) \right], \quad (20)$$

where $d_l^{(a)-Z'}$, $d_l^{(b)-Z'}$ can be obtained by replacing Z boson with a Z' boson in the expressions for $d_l^{(a)-Z}$, $d_l^{(b)-Z}$. Here, m_l denotes the mass of charged lepton l , and

$$\Phi(x) = \frac{1}{\sqrt{1-4x}} \left[\frac{\pi^2}{3} - \ln^2(x) + 2 \ln^2 \left(\frac{1 - \sqrt{1-4x}}{2} \right) - 4 \text{Li}_2 \left(\frac{1 - \sqrt{1-4x}}{2} \right) \right]. \quad (21)$$

Actually, the CPV parameters in the squark sector can also make contributions to d_μ , d_τ through the two-loop diagrams in Fig. 2, but they will make significant contributions to the neutron, mercury and heavy quark EDMs at the one-loop level, which are highly suppressed by the corresponding experimental upper bounds. Hence, We can neglect safely the contributions from the CPV parameters in the squark sector to d_μ , d_τ at the two-loop level. Finally, the EDM of charged lepton predicted dominantly in the B-LSSM can be calculated by

$$d_l = d_l^{(1)} + d_l^{(2)} + d_l^{(3)} + d_l^{(a)-\gamma} + d_l^{(b)-\gamma} + d_l^{(a)-Z} + d_l^{(b)-Z} + d_l^{(a)-Z'} + d_l^{(b)-Z'}. \quad (22)$$

III. NUMERICAL RESULTS OF d_μ , d_τ IN THE B-LSSM

In this section, we present the numerical predictions for d_μ and d_τ in the B-LSSM. For the relevant SM input parameters, we take $m_W = 80.385$ GeV, $m_Z = 90.1876$ GeV, $\alpha_{em}(m_Z) = 1/128.9$, $\alpha_s(m_Z) = 0.118$. The measured SM-like Higgs mass is taken as [69]

$$m_h = 125.09 \pm 0.24 \text{ GeV}. \quad (23)$$

The newly introduced Z' gauge boson, associated with the $U(1)_{B-L}$ gauge group, can also contribute via the two-loop diagrams. The ratio between the Z' mass, $M_{Z'} \approx \frac{1}{2}g_B u$, and its gauge coupling is subject to a strict lower bound at the 99% confidence level (CL) as [70–72]:

$$M_{Z'}/g_B \geq 6 \text{ TeV}. \quad (24)$$

For the other relevant parameters in the B-LSSM, we take the following benchmark points for simplicity to carry out the numerical computations

$$\begin{aligned} \tan \beta = 10, \tan \beta' = 1.15, g_B = 0.4, g_{YB} = -0.4, M_{Z'} = 5 \text{ TeV}, \\ m_{\tilde{l}} = m_{\tilde{e}} = m_{\tilde{\nu}} = \text{diag}(M_{\tilde{L}}, M_{\tilde{L}}, M_{\tilde{L}}), M_{\tilde{L}} = 0.5 \text{ TeV}, M_{\tilde{t}} = M_{\tilde{b}} = 2 \text{ TeV}, \\ M_1 = M_2 = \mu = 0.6e^{i\theta_\mu} \text{ TeV}, A_\mu = 0.1e^{i\theta_{A_\mu}} \text{ TeV}, A_\tau = 0.1e^{i\theta_{A_\tau}} \text{ TeV}, \\ M_{BB'} = 0.6e^{i\theta_{BB'}} \text{ TeV}, M_{BL} = 0.6e^{i\theta_{BL}} \text{ TeV}, \mu_\eta = 0.6e^{i\theta_{\mu_\eta}} \text{ TeV}, \\ \theta_\mu = 0, \theta_{A_\mu} = 0, \theta_{BB'} = 0, \theta_{BL} = 0, \theta_{\mu_\eta} = 0. \end{aligned} \quad (25)$$

The parameters in the first three lines also appeared in most SUSY models, while the ones in the penultimate line are the B-LSSM specific parameters. $M_{\tilde{t}}$, $M_{\tilde{b}}$ denote the stop and sbottom masses, respectively, which are used to calculate two-loop corrections to the SM-like Higgs boson mass. Unless we specify the parameter's value or the parameter as variable, Eq. (25) is taken as input in the numerical computations. The parameters fixed in Eq. (25) can well satisfy the constrains from LHC experimental data [73], high-precision measured $\text{Br}(\bar{B} \rightarrow X_s \gamma)$, $\text{Br}(B_s^0 \rightarrow \mu^+ \mu^-)$ [74], the direct searches of squarks, and the observed Higgs signal [75]. All flavor violating parameters are assumed to be zero without losing generality.

A. The effects of parameters in general SUSY models

Since the CPV parameters μ and A_l ($l = e, \mu, \tau$) are ubiquitous in most SUSY models, we first explore their effects on d_μ and d_τ . In Figs. 3(a) and 3(b), we set the CPV phases of the

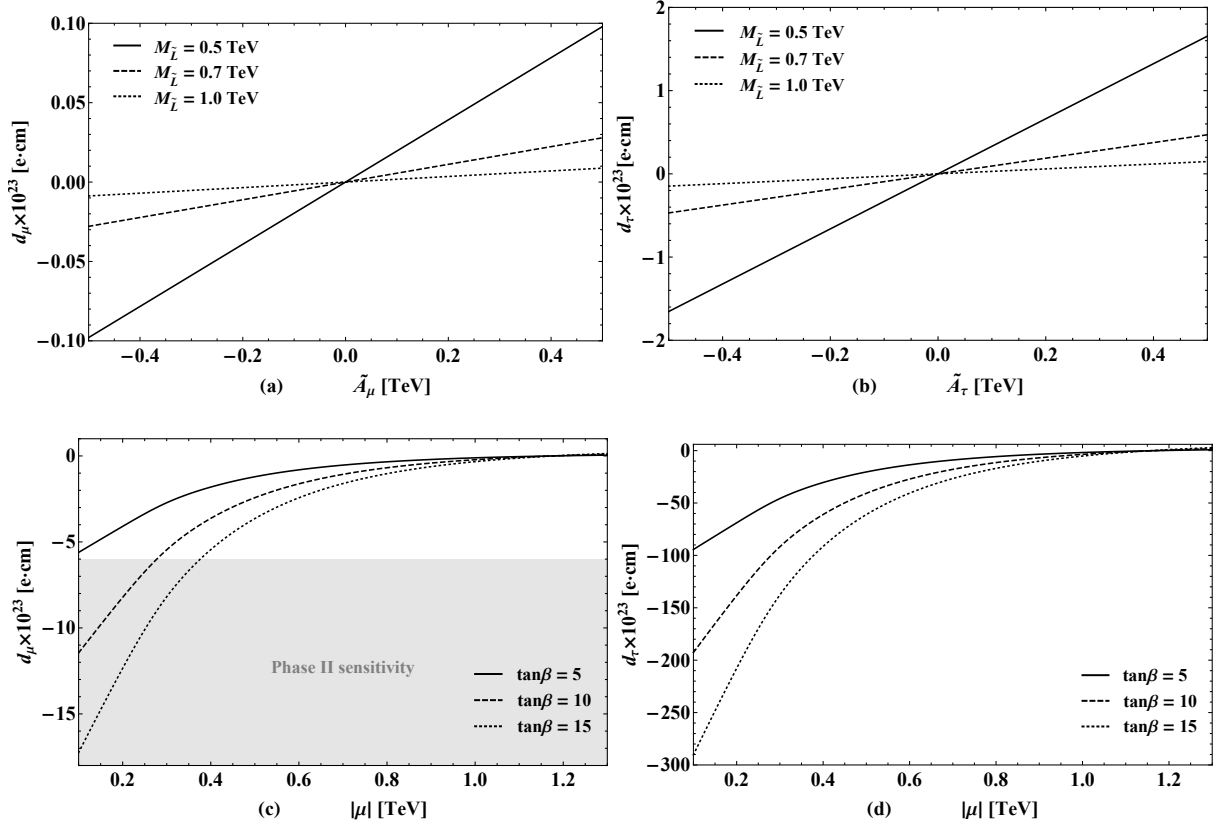


FIG. 3. The numerical results of d_μ versus \tilde{A}_μ (a) with $\theta_{A_\mu} = 0.5\pi$, d_τ versus \tilde{A}_τ (b) with $\theta_{A_\tau} = 0.5\pi$ and d_μ (c), d_τ (d) versus $|\mu|$ with $\theta_\mu = 0.5\pi$, the shaded area denotes the sensitivity can be reached in phase II.

trilinear scalar couplings to their maximal values, $\theta_{A_\mu} = \theta_{A_\tau} = 0.5\pi$. These figures illustrate the evolution of d_μ and d_τ as functions of the real parameters \tilde{A}_μ and \tilde{A}_τ , respectively, where $A_l \equiv \tilde{A}_l e^{i\theta_{A_l}}$. The solid, dashed, and dotted lines correspond to slepton mass parameters of $M_{\tilde{L}} = 0.5, 0.7, 1.0$ TeV, respectively.

Evidently, both d_μ and d_τ exhibit a clear linear dependence on their respective trilinear parameters \tilde{A}_l , vanishing exactly at $\tilde{A}_l = 0$. This behavior indicates that A_l serves as a primary direct CPV source for these loop-induced EDMs. Furthermore, as the slepton mass parameter $M_{\tilde{L}}$ increases, the slopes of these linear dependencies are strongly suppressed, clearly reflecting the decoupling effect of SUSY particles. A comparison between Figs. 3 (a) and (b) further reveals that the magnitude of d_τ is much larger than that of d_μ , because the A_l -induced left-right mixing term in the slepton mass matrix is proportional to the corresponding Yukawa couplings.

Figs. 3 (c) and (d) further investigate the CPV effects induced by the Higgsino mass parameter μ , whose CPV phase serves as a crucial source for generating the baryon asymmetry of the universe via electroweak baryogenesis. In these figures, we fix the CPV phase at $\theta_\mu = 0.5\pi$ and illustrate the dependence of the lepton EDMs on $|\mu|$ for different values of $\tan\beta$. The solid, dashed, and dotted lines denote the results of $\tan\beta = 5, 10, 15$, respectively. It can be seen that as $|\mu|$ increases, leading to heavier Higgsinos, the magnitudes of d_μ and d_τ asymptotically approach zero, which clearly confirms the decoupling behavior of heavy SUSY particles. On the other hand, the absolute magnitudes of the EDMs are significantly enhanced by larger values of $\tan\beta$. This is because a larger $\tan\beta$ substantially increases the Yukawa couplings of the down-type fermions, thereby greatly amplifying the theoretical predictions for the EDMs. Notably, the gray shaded area in Figs. 3 (c) indicates the anticipated sensitivity of the future Phase II experiment for d_μ . The numerical results demonstrate that in the parameter space characterized by a large $\tan\beta$ (e.g., $\tan\beta > 10$) and relatively light Higgsinos ($|\mu| \lesssim 0.4$ TeV), the theoretical prediction for d_μ falls entirely within the reach of Phase II.

B. The effects of B-LSSM specific parameters

As mentioned above, the B-LSSM introduces three specific CPV parameters: $M_{BB'}$, M_{BL} and μ_η . To see their contributions to d_μ , d_τ numerically, we take $\theta_{BB'} = 0.5\pi$ and plot d_μ and d_τ as functions of $\tilde{M}_{BB'}$ in Figs. 4(a) and 4(b), respectively. The solid, dashed, and dotted lines denote the results of $M_{\tilde{L}} = 0.5, 0.7, 1.0$ TeV, respectively. Similarly, d_μ , d_τ versus \tilde{M}_{BL} with $\theta_{BL} = 0.5\pi$ and $\tilde{\mu}_\eta$ with $\theta_{\mu_\eta} = 0.5\pi$ are also plotted. Here, we define $M_{BB'} \equiv \tilde{M}_{BB'} e^{i\theta_{BB'}}$, $M_{BL} \equiv \tilde{M}_{BL} e^{i\theta_{BL}}$, $\mu_\eta \equiv \tilde{\mu}_\eta e^{i\theta_{\mu_\eta}}$.

As can be seen from the picture that, the contributions from these B-LSSM specific CPV parameters are suppressed by heavy sleptons, because they contribute to d_μ and d_τ via the slepton-neutralino loop in Fig. 1 (3). Furthermore, their contributions also exhibit a strong flavor dependence, which is evident when comparing the results in the left column (Fig. 4 (a), (c), (e) for d_μ) with those in the right column (Fig. 4 (b), (d), (f) for d_τ). Similar to the reason mentioned above, the EDM operator $\bar{\psi}\sigma_{\mu\nu}\gamma_5\psi F^{\mu\nu}$ inherently dictates a chirality flip, its radiative corrections are typically proportional to the Yukawa coupling of the external fermion. Consequently, the theoretical expectation $d_\tau/d_\mu \sim m_\tau/m_\mu$ is excellently

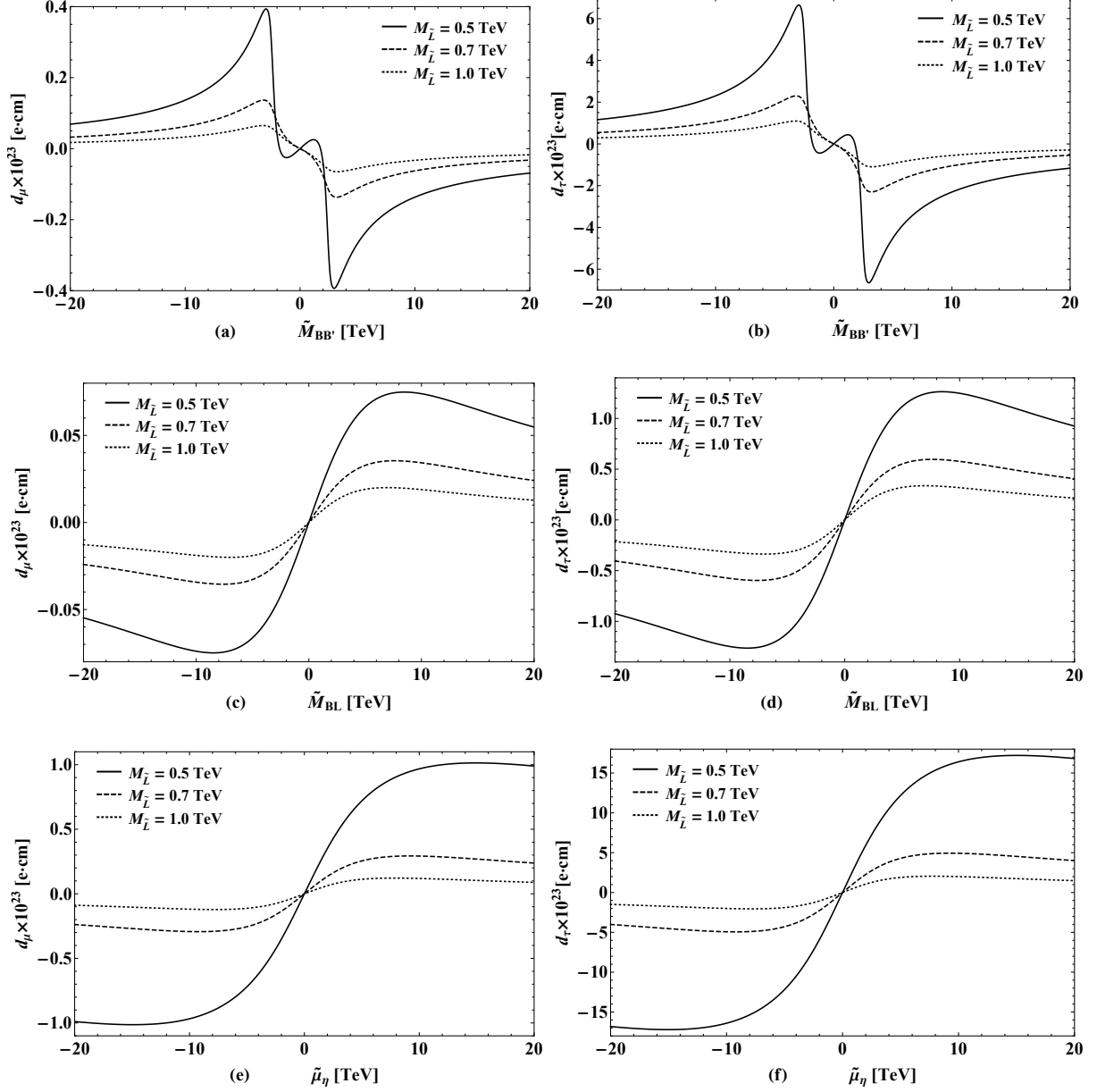


FIG. 4. Effects of B-LSSM specific CPV parameters on d_μ , d_τ . The panels display the dependence of d_μ and d_τ on $\tilde{M}_{BB'}$ (a, b), \tilde{M}_{BL} (c, d), and $\tilde{\mu}_\eta$ (e, f), with the respective CPV phases fixed at $\theta_{BB'} = 0.5\pi$, $\theta_{BL} = 0.5\pi$, $\theta_{\mu\eta} = 0.5\pi$. The solid, dashed, and dotted lines represent the slepton mass parameters $M_{\tilde{L}} = 0.5, 0.7, 1.0$ TeV, respectively.

corroborated by the numerical results.

In addition, Fig. 4 shows that the effects of $\tilde{M}_{BB'}$, \tilde{M}_{BL} , and $\tilde{\mu}_\eta$ on d_μ , d_τ exhibit entirely different asymptotic behaviors. The variation of the EDMs with respect to $\tilde{M}_{BB'}$ is highly

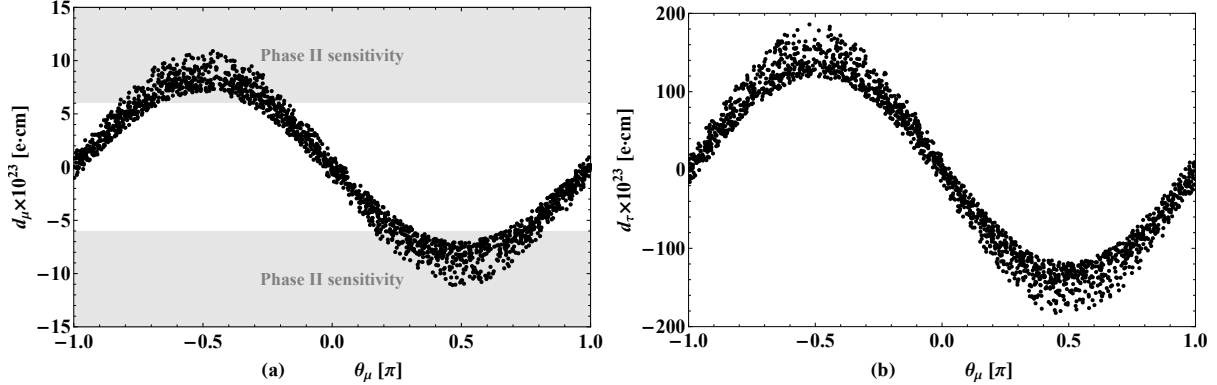


FIG. 5. Scatter plots of d_μ (a) and d_τ (b) versus the CPV phase θ_μ in the B-LSSM, incorporating the combined effects of all CPV phases. The fixed mass parameters are $|\mu| = 0.3$ TeV, $\tilde{M}_{BB'} = 3$ TeV, $\tilde{M}_{BL} = 8$ TeV, and $\tilde{\mu}_\eta = 10$ TeV. The points correspond to a random parameter scan over $\theta_\mu, \theta_{A_i}, \theta_{BB'}, \theta_{BL}, \theta_{\mu\eta} \in [-\pi, \pi]$. The gray shaded area denotes the sensitivity reach of the phase II experiment.

non-monotonic, with distinct extrema emerging around $|\tilde{M}_{BB'}| \approx 2$ and 3 TeV. $M_{BB'}$ describes the mixing effects between the superpartners of the gauge bosons corresponding to the two $U(1)$ gauge groups, it affects the numerical results in a much more complex manner than M_{BL} and μ_η . Figs. 4 (c-f) show that d_μ, d_τ initially increase as $|\tilde{M}_{BL}|$ and $|\tilde{\mu}_\eta|$ increase, reaching their respective maximum around $|\tilde{M}_{BL}| \approx 8$ TeV and $|\tilde{\mu}_\eta| \approx 14$ TeV. This behavior arises from an inherent physical interplay: while the CPV effects are initially enhanced by the larger parameter magnitudes, an excessively large mass scale ($|\tilde{M}_{BL}|$ or $|\tilde{\mu}_\eta|$) yields heavy neutralinos, which ultimately suppress the total contributions in accordance with the decoupling theorem. This decoupling-induced suppression at large mass scales is also responsible for the asymptotic decay observed at large $|\tilde{M}_{BB'}|$ in Figs. 4(a) and 4(b).

C. The combined predictions

In this subsection, we present the theoretical predictions for d_μ and d_τ by considering the combined effects of all possible CPV parameters. To illustrate regions of the parameter space with substantial EDM predictions, we adopt the benchmark values $|\mu| = 0.3$ TeV, $\tilde{M}_{BB'} = 3$ TeV, $\tilde{M}_{BL} = 8$ TeV, and $\tilde{\mu}_\eta = 10$ TeV based on the preceding analysis. We then

perform a random scan over the following parameter space:

$$\theta_\mu \in [-\pi, \pi], \theta_{A_l} \in [-\pi, \pi], \theta_{BB'} \in [-\pi, \pi], \theta_{BL} \in [-\pi, \pi], \theta_{\mu\eta} \in [-\pi, \pi], \quad (26)$$

and plot d_μ and d_τ versus θ_μ in Figs. 5 (a) and Fig. 5 (b), respectively.

As clearly observed in Fig. 5 (a) and Fig. 5 (b), the lepton EDMs d_μ and d_τ exhibit a strong, nearly sinusoidal oscillatory dependence on the phase θ_μ . Both reach their peak magnitudes at $\theta_\mu \approx \pm 0.5\pi$, whereas the corresponding EDM predictions approach zero in the vicinity of $\theta_\mu \approx 0$ and $\pm\pi$. This behavior indicates that, within the selected parameter space, the CPV phase θ_μ of the Higgsino mass parameter μ provides the dominant contributions to d_μ and d_τ . Furthermore, the scatter points do not follow a single uniform curve but instead form a “band” with a specific vertical width. The band widths for d_μ in Fig. 5 (a) and d_τ in Fig. 5 (b) are approximately $\Delta d_\mu \sim 3 \times 10^{-23}$ e·cm and $\Delta d_\tau \sim 50 \times 10^{-23}$ e·cm, respectively. Since these scatter points mainly results from the B-LSSM specific CPV parameters, it indicates they can also affect the theoretical predictions on d_μ , d_τ significantly, although θ_μ affects d_μ , d_τ dominantly.

Numerically, the model yields a maximum prediction of $|d_\mu| \sim 1.0 \times 10^{-22}$ e·cm, while the maximum $|d_\tau|$ is substantially amplified to $\sim 1.8 \times 10^{-21}$ e·cm. The gray shaded area highlighted in Fig. 5 (a) indicates the anticipated reach of the Phase II experiment for the muon EDM ($|d_\mu| \gtrsim 6 \times 10^{-23}$ e·cm). As shown by the numerical results, the majority of the theoretical scatter points land inside this accessible region for large CPV phases within $0.25\pi \lesssim |\theta_\mu| \lesssim 0.75\pi$. This leads to a highly significant phenomenological conclusion: the Phase II experiment will be sensitive enough to either verify or rule out regions of the B-LSSM parameter space featuring substantial θ_μ phases. Conversely, a continued null result from future experiments would tightly restrict θ_μ to a narrow interval around zero, unless severe fine-tuning via multi-parameter destructive interference is invoked to reconcile the model with the experimental data.

IV. SUMMARY

In this work, we present a phenomenological study on the EDMs of the muon (d_μ) and tau (d_τ) within the framework of the B-LSSM. We incorporate both the general SUSY CPV sources (μ , A_l) and the B-LSSM specific CPV parameters ($M_{BB'}$, M_{BL} , μ_η), systematically

analyzing their loop-induced contributions to d_μ , d_τ . We found that while the decoupling theorem is strictly and immediately manifested for heavy sleptons and Higgsinos, the B-LSSM specific parameters $M_{BB'}$, M_{BL} , μ_η exhibit more complex behaviors. For these specific parameters, the decoupling suppression only begins to dominate the numerical results when their respective mass scales become exceedingly large (e.g., $\gtrsim 20$ TeV).

Furthermore, our numerical scans reveal that the theoretical predictions for d_μ and d_τ exhibit a pronounced sinusoidal dependence on θ_μ , indicating that the CPV phase of the Higgsino mass parameter μ provides the dominant contributions to d_μ and d_τ . Although the B-LSSM specific CPV parameters provide subleading corrections, they can still significantly modulate the overall theoretical predictions. The B-LSSM naturally yields a muon EDM on the order of $\mathcal{O}(10^{-22}) e \cdot \text{cm}$, which substantially overlaps with the projected detection sensitivities of the recently proposed Phase II experiments. While $|d_\tau|$ can reach about $10^{-21} e \cdot \text{cm}$, such values remain challenging to observe in the near future.

ACKNOWLEDGMENTS

The work has been supported by the National Natural Science Foundation of China (NNSFC) with Grants No. 12075074, No. 12235008, the Hebei Natural Science Foundation for Distinguished Young Scholars with Grant No. A2023201041 and the youth top-notch talent support program of the Hebei Province.

Appendix A: Constants $C_{XYZ}^{L(R)}$ appear in our calculation

The used coupling constants in the computations are

$$C_{\tilde{\chi}_i^\pm \nu_{\text{odd},j}}^L = -\frac{1}{\sqrt{2}} U_{i2}^* \sum_{b=1}^3 Z_{jb}^{I,*} \sum_{a=1}^3 U_{R,la}^{e,*} Y_{e,ab} \quad (\text{A1})$$

$$C_{\bar{l}\chi_i^\pm\nu_{\text{odd},j}}^R = \frac{1}{\sqrt{2}} \left(g_2 \sum_{a=1}^3 Z_{ja}^{I,*} U_{L,la}^e V_{i1} - \sum_{b=1}^3 \sum_{a=1}^3 Y_{\nu,ab}^* Z_{j,3+a}^{I,*} U_{L,lb}^e V_{i2} \right) \quad (\text{A2})$$

$$C_{\bar{l}\chi_i^\pm\nu_{\text{even},j}}^L = \frac{1}{\sqrt{2}} U_{i2}^* \sum_{b=1}^3 Z_{jb}^{R,*} \sum_{a=1}^3 U_{R,la}^{e,*} Y_{e,ab} \quad (\text{A3})$$

$$C_{\bar{l}\chi_i^\pm\nu_{\text{even},j}}^R = \frac{1}{\sqrt{2}} \left(-g_2 \sum_{a=1}^3 Z_{ja}^{R,*} U_{L,la}^e V_{i1} + \sum_{b=1}^3 \sum_{a=1}^3 Y_{\nu,ab}^* Z_{j,3+a}^{R,*} U_{L,lb}^e V_{i2} \right) \quad (\text{A4})$$

$$C_{h_k\bar{\chi}_i^\pm\chi_j^\pm} = -\frac{1}{\sqrt{2}} g_2 (U_{j1}^* V_{i2}^* Z_{k2}^H + U_{j2}^* V_{i1}^* Z_{k1}^H), \quad C_{h_k\bar{l}}^* = -\frac{1}{\sqrt{2}} Y_{e,ll} Z_{k1}^H \quad (\text{A5})$$

$$C_{Z\bar{l}}^L = \frac{1}{2} \left(-g_1 \cos \Theta'_W \sin \Theta_W + g_2 \cos \Theta_W \cos \Theta'_W + (g_{YB} + g_B) \sin \Theta'_W \right) \quad (\text{A6})$$

$$C_{Z\bar{l}}^R = -\frac{1}{2} \left(2g_1 \cos \Theta'_W \sin \Theta_W - (2g_{YB} + g_B) \sin \Theta'_W \right) \quad (\text{A7})$$

$$C_{Z'\bar{l}}^L = \frac{1}{2} \left((g_1 \sin \Theta_W - g_2 \cos \Theta_W) \sin \Theta'_W + (g_{YB} + g_B) \cos \Theta'_W \right) \quad (\text{A8})$$

$$C_{Z'\bar{l}}^R = \frac{1}{2} \left(2g_1 \sin \Theta_W \sin \Theta'_W + (2g_{YB} + g_B) \cos \Theta'_W \right) \quad (\text{A9})$$

$$C_{Z\bar{\chi}_i^\pm\chi_j^\pm}^L = \frac{1}{2} \left(2g_2 U_{j1}^* \cos \Theta_W \cos \Theta'_W U_{i1} + U_{j2}^* (-g_1 \cos \Theta'_W \sin \Theta_W + g_2 \cos \Theta_W \cos \Theta'_W + g_{YB} \sin \Theta'_W) U_{i2} \right) \quad (\text{A10})$$

$$C_{Z\bar{\chi}_i^\pm\chi_j^\pm}^R = \frac{1}{2} \left(2g_2 V_{i1}^* \cos \Theta_W \cos \Theta'_W V_{j1} + V_{i2}^* (-g_1 \cos \Theta'_W \sin \Theta_W + g_2 \cos \Theta_W \cos \Theta'_W + g_{YB} \sin \Theta'_W) V_{j2} \right) \quad (\text{A11})$$

$$C_{Z'\bar{\chi}_i^\pm\chi_j^\pm}^L = -\frac{1}{2} \left(2g_2 U_{j1}^* \cos \Theta_W \sin \Theta'_W U_{i1} - U_{j2}^* ((g_1 \sin \Theta_W - g_2 \cos \Theta_W) \sin \Theta'_W + g_{YB} \cos \Theta'_W) U_{i2} \right) \quad (\text{A12})$$

$$C_{Z'\bar{\chi}_i^\pm\chi_j^\pm}^R = -\frac{1}{2} \left(2g_2 V_{i1}^* \cos \Theta_W \sin \Theta'_W V_{j1} - V_{i2}^* ((g_1 \sin \Theta_W - g_2 \cos \Theta_W) \sin \Theta'_W + g_{YB} \cos \Theta'_W) V_{j2} \right) \quad (\text{A13})$$

$$C_{\bar{l}\chi_i^0\bar{E}_j}^L = \left(-\frac{1}{\sqrt{2}} 2g_1 N_{i1}^* \sum_{a=1}^3 Z_{j,3+a}^{E,*} U_{R,la}^{e,*} - \frac{1}{\sqrt{2}} (2g_{YB} + g_B) N_{i5}^* \sum_{a=1}^3 Z_{j,3+a}^{E,*} U_{R,la}^{e,*} - N_{i3}^* \sum_{b=1}^3 Z_{jb}^{E,*} \sum_{a=1}^3 U_{R,la}^{e,*} Y_{e,ab} \right) \quad (\text{A14})$$

$$C_{\tilde{\chi}_i^0 \tilde{E}_j}^R = \frac{1}{2} \left(-2 \sum_{b=1}^3 \sum_{a=1}^3 Y_{e,ab}^* Z_{j,3+a}^{E,*} U_{L,lb}^e N_{i3} + \sqrt{2} \sum_{a=1}^3 Z_{ja}^{E,*} U_{L,la}^e (g_1 N_{i1} + g_2 N_{i2} + (g_{YB} + g_B) N_{i5}) \right) \quad (\text{A15})$$

$$C_{h_k \tilde{E}_i \tilde{E}_i} = \frac{1}{4} \left(-2 \left(\sqrt{2} \sum_{b=1}^3 Z_{ib}^{E,*} \sum_{a=1}^3 Z_{i,3+a}^E T_{e,ab} Z_{k1}^H + \sqrt{2} \sum_{b=1}^3 \sum_{a=1}^3 Z_{i,3+a}^{E,*} T_{e,ab}^* Z_{ib}^E Z_{k1}^H \right. \right. \\ + 2v_1 \sum_{c=1}^3 Z_{i,3+c}^{E,*} \sum_{b=1}^3 \sum_{a=1}^3 Y_{e,ca} Y_{e,ba} Z_{i,3+b}^E Z_{k1}^H + 2v_1 \sum_{c=1}^3 \sum_{b=1}^3 Z_{ib}^{E,*} \sum_{a=1}^3 Y_{e,ac}^* Y_{e,ab} Z_{ic}^E Z_{k1}^H \\ - \sqrt{2} \mu^* \sum_{b=1}^3 Z_{ib}^{E,*} \sum_{a=1}^3 Y_{e,ab} Z_{i,3+a}^E Z_{k2}^H - \sqrt{2} \mu \sum_{b=1}^3 \sum_{a=1}^3 Y_{e,ab}^* Z_{i,3+a}^{E,*} Z_{ib}^E Z_{k2}^H \left. \right) \\ + \sum_{a=1}^3 Z_{i,3+a}^{E,*} Z_{i,3+a}^E \left((2g_1^2 + g_{YB}(2g_{YB} + g_B)) v_1 Z_{k1}^H \right. \\ - (2g_1^2 + g_{YB}(2g_{YB} + g_B)) v_2 Z_{k2}^H + 2(2g_{YB}g_B + g_B^2) (-u_{\tilde{\eta}} Z_{k4}^H + u_{\tilde{\eta}} Z_{k3}^H) \left. \right) \\ + \sum_{a=1}^3 Z_{ia}^{E,*} Z_{ia}^E \left(-(-g_2^2 + g_{YB}g_B + g_1^2 + g_{YB}^2) v_1 Z_{k1}^H \right. \\ \left. + (-g_2^2 + g_{YB}g_B + g_1^2 + g_{YB}^2) v_2 Z_{k2}^H - 2(g_{YB}g_B + g_B^2) (-u_{\tilde{\eta}} Z_{k4}^H + u_{\tilde{\eta}} Z_{k3}^H) \right) \left. \right) \quad (\text{A16})$$

$$C_{Z \tilde{E}_i \tilde{E}_i} = \frac{1}{2} \left(\left(-g_1 \cos \Theta'_W \sin \Theta_W + g_2 \cos \Theta_W \cos \Theta'_W + (g_{YB} + g_B) \sin \Theta'_W \right) \sum_{a=1}^3 Z_{ia}^{E,*} Z_{ia}^E \right. \\ \left. + \left(-2g_1 \cos \Theta'_W \sin \Theta_W + (2g_{YB} + g_B) \sin \Theta'_W \right) \sum_{a=1}^3 Z_{i,3+a}^{E,*} Z_{i,3+a}^E \right) \quad (\text{A17})$$

$$C_{Z' \tilde{E}_i \tilde{E}_i} = \frac{1}{2} \left(\left((g_1 \sin \Theta_W - g_2 \cos \Theta_W) \sin \Theta'_W + (g_{YB} + g_B) \cos \Theta'_W \right) \sum_{a=1}^3 Z_{ia}^{E,*} Z_{ia}^E \right. \\ \left. + \left(2g_1 \sin \Theta_W \sin \Theta'_W + (2g_{YB} + g_B) \cos \Theta'_W \right) \sum_{a=1}^3 Z_{i,3+a}^{E,*} Z_{i,3+a}^E \right) \quad (\text{A18})$$

In the above expressions, we have $Y_e = \text{diag} \sqrt{2}(m_e, m_\mu, m_\tau)/v_1$, $U_L^e = U_R^e = \text{diag}(1, 1, 1)$, and the matrices U, V, Z^E, Z^I, Z^R , and N are the rotation matrices that relate the gauge eigenstates to the mass eigenstates. Their explicit definitions are as follows:

$$U^* m_{\tilde{\chi}^-} V^\dagger = m_{\tilde{\chi}^-}^{dia}, \quad (\text{A19})$$

$$Z^E m_{\tilde{l}}^2 Z^{E,\dagger} = m_{2,\tilde{l}}^{dia}, \quad (\text{A20})$$

$$Z^I m_{\tilde{\nu}_{\text{odd}}}^2 Z^{I,\dagger} = m_{2,m_{\tilde{\nu}_{\text{odd}}}}^{dia}, \quad (\text{A21})$$

$$Z^R m_{\tilde{\nu}_{\text{even}}}^2 Z^{R,\dagger} = m_{2,m_{\tilde{\nu}_{\text{even}}}}^{dia}, \quad (\text{A22})$$

$$N^* m_{\tilde{\chi}^0} N^\dagger = m_{\tilde{\chi}^0}^{dia}, \quad (\text{A23})$$

where $m_{\tilde{\chi}^-}$ is the mass matrix of charginos.

-
- [1] J. H. Christenson, J. W. Cronin, V. L. Fitch, and R. Turlay, *Phys. Rev. Lett.* **13**, 138 (1964).
- [2] K. Abe *et al.* (Belle), *Phys. Rev. Lett.* **87**, 091802 (2001), arXiv:hep-ex/0107061.
- [3] B. Aubert *et al.* (BaBar), *Phys. Rev. Lett.* **89**, 201802 (2002), arXiv:hep-ex/0207042.
- [4] R. Cooke, M. Pettini, R. A. Jorgenson, M. T. Murphy, and C. C. Steidel, *Astrophys. J.* **781**, 31 (2014), arXiv:1308.3240 [astro-ph.CO].
- [5] P. A. R. Ade *et al.* (Planck), *Astron. Astrophys.* **594**, A13 (2016), arXiv:1502.01589 [astro-ph.CO].
- [6] M. E. Pospelov and I. B. Khriplovich, *Sov. J. Nucl. Phys.* **53**, 638 (1991).
- [7] M. Pospelov and A. Ritz, *Phys. Rev. D* **89**, 056006 (2014), arXiv:1311.5537 [hep-ph].
- [8] Y. Yamaguchi and N. Yamanaka, *Phys. Rev. Lett.* **125**, 241802 (2020), arXiv:2003.08195 [hep-ph].
- [9] Y. Yamaguchi and N. Yamanaka, *Phys. Rev. D* **103**, 013001 (2021), arXiv:2006.00281 [hep-ph].
- [10] Y. Ema, T. Gao, and M. Pospelov, *Phys. Rev. Lett.* **129**, 231801 (2022), arXiv:2202.10524 [hep-ph].
- [11] J. Engel, M. J. Ramsey-Musolf, and U. van Kolck, *Prog. Part. Nucl. Phys.* **71**, 21 (2013), arXiv:1303.2371 [nucl-th].
- [12] T. Chupp, P. Fierlinger, M. Ramsey-Musolf, and J. Singh, *Rev. Mod. Phys.* **91**, 015001 (2019), arXiv:1710.02504 [physics.atom-ph].
- [13] S. Abel, S. Khalil, and O. Lebedev, *Nucl. Phys. B* **606**, 151 (2001), arXiv:hep-ph/0103320.
- [14] T. Ibrahim, *Phys. Rev. D* **64**, 035009 (2001), arXiv:hep-ph/0102218.

- [15] C. Cesarotti, Q. Lu, Y. Nakai, A. Parikh, and M. Reece, *JHEP* **05**, 059 (2019), arXiv:1810.07736 [hep-ph].
- [16] A. Maiezza and M. Nemevšek, *Phys. Rev. D* **90**, 095002 (2014), arXiv:1407.3678 [hep-ph].
- [17] S. Bertolini, A. Maiezza, and F. Nesti, *Phys. Rev. D* **101**, 035036 (2020), arXiv:1911.09472 [hep-ph].
- [18] W. Altmannshofer, S. Gori, N. Hamer, and H. H. Patel, *Phys. Rev. D* **102**, 115042 (2020), arXiv:2009.01258 [hep-ph].
- [19] S. M. Barr and A. Zee, *Phys. Rev. Lett.* **65**, 21 (1990), [Erratum: *Phys.Rev.Lett.* 65, 2920 (1990)].
- [20] E. J. Chun, J. Kim, and T. Mondal, *JHEP* **12**, 068 (2019), arXiv:1906.00612 [hep-ph].
- [21] S. F. King, M. Muhlleitner, R. Nevzorov, and K. Walz, *Nucl. Phys. B* **901**, 526 (2015), arXiv:1508.03255 [hep-ph].
- [22] D. Chang, W.-F. Chang, M. Frank, and W.-Y. Keung, *Phys. Rev. D* **62**, 095002 (2000), arXiv:hep-ph/0004170.
- [23] N. Yamanaka, T. Sato, and T. Kubota, *Phys. Rev. D* **85**, 117701 (2012), arXiv:1202.0106 [hep-ph].
- [24] N. Yamanaka, *Phys. Rev. D* **86**, 075029 (2012), arXiv:1208.4521 [hep-ph].
- [25] N. Yamanaka, T. Sato, and T. Kubota, *Phys. Rev. D* **87**, 115011 (2013), arXiv:1212.6833 [hep-ph].
- [26] S. Khalil and H. Okada, *Phys. Rev. D* **79**, 083510 (2009), arXiv:0810.4573 [hep-ph].
- [27] A. Elsayed, S. Khalil, and S. Moretti, *Phys. Lett. B* **715**, 208 (2012), arXiv:1106.2130 [hep-ph].
- [28] A. Elsayed, S. Khalil, S. Moretti, and A. Moursy, *Phys. Rev. D* **87**, 053010 (2013), arXiv:1211.0644 [hep-ph].
- [29] W. Abdallah, A. Hammad, S. Khalil, and S. Moretti, *Phys. Rev. D* **95**, 055019 (2017), arXiv:1608.07500 [hep-ph].
- [30] S. Khalil and S. Moretti, *Rept. Prog. Phys.* **80**, 036201 (2017), arXiv:1503.08162 [hep-ph].
- [31] L. Delle Rose, S. Khalil, S. J. D. King, S. Kulkarni, C. Marzo, S. Moretti, and C. S. Un, *JHEP* **07**, 100 (2018), arXiv:1712.05232 [hep-ph].
- [32] J.-L. Yang, T.-F. Feng, and H.-B. Zhang, *J. Phys. G* **47**, 055004 (2020), arXiv:2003.09781 [hep-ph].
- [33] J.-L. Yang, H.-B. Zhang, C.-X. Liu, X.-X. Dong, and T.-F. Feng, *JHEP* **08**, 086 (2021),

- arXiv:2104.03542 [hep-ph].
- [34] A. A. Abdelalim, B. Das, S. Khalil, and S. Moretti, Nucl. Phys. B **985**, 116013 (2022), arXiv:2012.04952 [hep-ph].
- [35] S. Khalil, LHEP **2023**, 454 (2023).
- [36] J.-L. Yang, T.-F. Feng, S.-K. Cui, C.-X. Liu, W. Li, and H.-B. Zhang, JHEP **04**, 013 (2020), arXiv:1910.05868 [hep-ph].
- [37] J.-L. Yang, T.-F. Feng, and H.-B. Zhang, Eur. Phys. J. C **80**, 210 (2020), arXiv:2002.09313 [hep-ph].
- [38] K. Inami *et al.* (Belle), JHEP **04**, 110 (2022), arXiv:2108.11543 [hep-ex].
- [39] G. W. Bennett *et al.* (Muon (g-2)), Phys. Rev. D **80**, 052008 (2009), arXiv:0811.1207 [hep-ex].
- [40] T. S. Roussy *et al.*, Science **381**, adg4084 (2023), arXiv:2212.11841 [physics.atom-ph].
- [41] T. Abe *et al.* (Belle-II), (2010), arXiv:1011.0352 [physics.ins-det].
- [42] W. Altmannshofer *et al.* (Belle-II), PTEP **2019**, 123C01 (2019), [Erratum: PTEP 2020, 029201 (2020)], arXiv:1808.10567 [hep-ex].
- [43] H. Aihara *et al.*, (2024), arXiv:2406.19421 [hep-ex].
- [44] M. Ablikim *et al.* (BESIII), Nucl. Instrum. Meth. A **614**, 345 (2010), arXiv:0911.4960 [physics.ins-det].
- [45] M. Ablikim *et al.* (BESIII), Chin. Phys. C **44**, 040001 (2020), arXiv:1912.05983 [hep-ex].
- [46] W. Bernreuther, L. Chen, and O. Nachtmann, Phys. Rev. D **104**, 115002 (2021), arXiv:2108.13106 [hep-ph].
- [47] M. Dong *et al.* (CEPC Study Group), (2018), arXiv:1811.10545 [hep-ex].
- [48] H. Cheng *et al.* (CEPC Physics Study Group), in *Snowmass 2021* (2022) arXiv:2205.08553 [hep-ph].
- [49] D. Bodrov, Int. J. Mod. Phys. A **39**, 2442006 (2024), arXiv:2405.16512 [hep-ex].
- [50] A. Crivellin, M. Hoferichter, and J. M. Roney, Phys. Rev. D **106**, 093007 (2022), arXiv:2111.10378 [hep-ph].
- [51] A. Crivellin, M. Hoferichter, and P. Schmidt-Wellenburg, Phys. Rev. D **98**, 113002 (2018), arXiv:1807.11484 [hep-ph].
- [52] A. Adelman *et al.*, Eur. Phys. J. C **85**, 622 (2025), arXiv:2501.18979 [hep-ex].
- [53] Y. Nakai, Y. Shigekami, P. Sun, and Z. Zhang, Phys. Rev. D **113**, 035001 (2026), arXiv:2508.05935 [hep-ph].

- [54] Z.-L. Huang, X.-Y. Du, X.-G. He, C.-W. Liu, and Z.-Y. Zou, *Chin. Phys. Lett.* **43**, 030201 (2026), arXiv:2510.23348 [hep-ph].
- [55] K. Deka, M. Losada, and Y. Nir, *JHEP* **03**, 065 (2026), arXiv:2511.21828 [hep-ph].
- [56] P. Minkowski, *Phys. Lett. B* **67**, 421 (1977).
- [57] S. Weinberg, *Phys. Rev. Lett.* **43**, 1566 (1979).
- [58] J.-L. Yang, Z.-J. Yang, X.-Y. Yang, H.-B. Zhang, and T.-F. Feng, *Eur. Phys. J. C* **83**, 1073 (2023).
- [59] B. Holdom, *Phys. Lett. B* **166**, 196 (1986).
- [60] T. Matsuoka and D. Suematsu, *Prog. Theor. Phys.* **76**, 901 (1986).
- [61] F. del Aguila, J. A. Gonzalez, and M. Quiros, *Nucl. Phys. B* **307**, 571 (1988).
- [62] F. del Aguila, G. D. Coughlan, and M. Quiros, *Nucl. Phys. B* **307**, 633 (1988), [Erratum: *Nucl.Phys.B* 312, 751 (1989)].
- [63] R. Foot and X.-G. He, *Phys. Lett. B* **267**, 509 (1991).
- [64] K. S. Babu, C. F. Kolda, and J. March-Russell, *Phys. Rev. D* **57**, 6788 (1998), arXiv:hep-ph/9710441.
- [65] J.-L. Yang, M.-H. Guo, W.-H. Zhang, H.-B. Zhang, and T.-F. Feng, (2024), arXiv:2406.01926 [hep-ph].
- [66] K. Cheung, O. C. W. Kong, and J. S. Lee, *JHEP* **06**, 020 (2009), arXiv:0904.4352 [hep-ph].
- [67] N. Yamanaka, *Phys. Rev. D* **108**, 095004 (2023), arXiv:1212.5800 [hep-ph].
- [68] W. Altmannshofer, P. S. B. Dev, A. Soni, and F. Xu, *JHEP* **01**, 153 (2026), arXiv:2507.23722 [hep-ph].
- [69] S. Navas *et al.* (Particle Data Group), *Phys. Rev. D* **110**, 030001 (2024).
- [70] M. Carena, A. Daleo, B. A. Dobrescu, and T. M. P. Tait, *Phys. Rev. D* **70**, 093009 (2004), arXiv:hep-ph/0408098.
- [71] G. Cacciapaglia, C. Csaki, G. Marandella, and A. Strumia, *Phys. Rev. D* **74**, 033011 (2006), arXiv:hep-ph/0604111.
- [72] ATLAS Collaboration, ATLAS-CONF-2016-045 (2016).
- [73] L. Basso, *Adv. High Energy Phys.* **2015**, 980687 (2015), arXiv:1504.05328 [hep-ph].
- [74] J.-L. Yang, T.-F. Feng, S.-M. Zhao, R.-F. Zhu, X.-Y. Yang, and H.-B. Zhang, *Eur. Phys. J. C* **78**, 714 (2018), arXiv:1803.09904 [hep-ph].
- [75] C. S. Un and O. Ozdal, *Phys. Rev. D* **93**, 055024 (2016), arXiv:1601.02494 [hep-ph].